OUKA
The University of Osaka
Institutional Knowledge Archive

Title	Amyloid Fibril Formation in the Context of Full-length Protein : EFFECTS OF PROLINE MUTATIONS ON THE AMYLOID FIBRIL FORMATION OF β2-MICROGLOBULIN
Author(s)	Chiba, Takeshi; Hagihara, Yoshihisa; Higurashi, Takashi et al.
Citation	Journal of Biological Chemistry. 2003, 278(47), p. 47016-47024
Version Type	VoR
URL	https://hdl.handle.net/11094/71299
rights	
Note	

The University of Osaka Institutional Knowledge Archive : OUKA

https://ir.library.osaka-u.ac.jp/

The University of Osaka

THE JOURNAL OF BIOLOGICAL CHEMISTRY
Vol. 278, No. 47, Issue of November 21, pp. 47016–47024, 2003
Printed in U.S.A.
© 2003 by The American Society for Biochemistry and Molecular Biology, Inc.

Amyloid Fibril Formation in the Context of Full-length Protein

EFFECTS OF PROLINE MUTATIONS ON THE AMYLOID FIBRIL FORMATION OF β_2-MICROGLOBULIN*

Received for publication, April 29, 2003, and in revised form, July 31, 2003
Published, JBC Papers in Press, September 4, 2003, DOI 10.1074/jbc.M304473200

Takeshi Chiba‡§, Yoshihisa Hagihara§¶, Takashi Higurashi‡, Kazuhiro Hasegawa‖, Hironobu Naiki‖, and Yuji Goto‡**

From the ‡Institute for Protein Research, Osaka University, and CREST, Japan Science and Technology Corp., Yamadaoka 3-2, Suita, Osaka 565-0871, Japan, ¶Special Division for Human Life Technology, National Institute of Advanced Industrial Science and Technology, 1-8-31 Midorigaoka, Ikeda, Osaka 563-8577, Japan, and ‖Department of Pathology, Fukui Medical University, and CREST, Japan Science and Technology Corp., Matsuoka, Fukui 910-1193, Japan

β_2-Microglobulin (β2-m), a typical immunoglobulin domain made of seven β-strands, is a major component of amyloid fibrils formed in dialysis-related amyloidosis. To understand the mechanism of amyloid fibril formation in the context of full-length protein, we prepared various mutants in which proline (Pro) was introduced to each of the seven β-strands of β2-m. The mutations affected the amyloidogenic potential of β2-m to various degrees. In particular, the L23P, H51P, and V82P mutations significantly retarded fibril extension at pH 2.5. Among these, only L23P is included in the known "minimal" peptide sequence, which can form amyloid fibrils when isolated as a short peptide. This indicates that the residues in regions other than the minimal sequence, such as H51P and V82P, determine the amyloidogenic potential in the full-length protein. To further clarify the mutational effects, we measured their stability against guanidine hydrochloride of the native state at pH 8.0 and the amyloid fibrils at pH 2.5. The amyloidogenicity of mutants showed a significant correlation with the stability of the amyloid fibrils, and little correlation was observed with that of the native state. It has been proposed that the stability of the native state and the unfolding rate to the amyloidogenic precursor as well as the conformational preference of the denatured state determine the amyloidogenicity of the proteins. The present results reveal that, in addition, stability of the amyloid fibrils is a key factor determining the amyloidogenic potential of the proteins.

More than 20 diseases are related to the deposition of insoluble amyloid fibrils (1–3). In some cases, such as Alzheimer's disease, fibril components are the truncated relatively short fragments of amyloid precursor proteins. In other types of amyloidosis, such as familial amyloid polyneuropathy and dialysis-related amyloidosis, amyloid fibrils are made of the entire part of the originally globular proteins. For these proteins, it has been shown that short peptides, called minimal (or essential) sequences, can also form amyloid fibrils (4–7). These findings raise the question of whether regions other than the minimal sequence affect the amyloid fibril formation.

For many amyloidogenic globular proteins, destabilization of the native globular state by mutation or by introduction of unstable conditions is highly correlated with the formation of amyloid fibrils, suggesting that the denaturation or unfolding of the native state is the critical event in triggering amyloid formation (8–12). A study with a series of transthyretin mutants revealed that the unfolding rate rather than the thermodynamic stability is an important factor determining amyloidogenicity (13). Alternatively, because the non-native state is an intermediate or precursor of amyloid fibril formation, residues other than the minimal region can control amyloid fibril formation by affecting the conformational properties of the non-native state. Consistent with this, recent studies with various mutants of acylphosphatase demonstrated that the hydrophobicity and β-sheet propensity of the key regions, which are distinct from those parts important for protein folding, as well as the net charge of the protein are the critical factors for aggregation (14, 15). Moreover, it is likely that mutations affecting the stability of the amyloid fibrils also determine the amyloidogenicity of proteins.

Dialysis-related amyloidosis is a common and serious complication in patients receiving long term hemodialysis for more than 10 years (16–18). In this disease, full-length β_2-microglobulin (β2-m)[1] is a major structural component of amyloid fibrils (16). The straight needle-like amyloid fibrils can be formed *in vitro* by the seed-dependent extension reaction at pH 2.5, in which monomeric β2-m is added to the end(s) of seed fibrils (19). The similar amyloid fibrils are formed spontaneously with a lag phase at pH 2.5 and low ionic strength (20). Kozhukh *et al.* (7) find that the isolated 22-residue K3 peptide, Ser-20–Lys-41 (Fig. 1*A*), forms amyloid fibrils, suggesting that this peptide includes the initiation and minimal region of amyloid fibrils. Recently, we identified that an 11-residue peptide, Asn-21–His-31, in the K3 region also forms amyloid fibrils (21). In addition, Jones *et al.* (5) identify another peptide, Asp-59–Thr-71, forms amyloid fibrils.

In amyloid fibrils of β2-m, more than 50% of amide protons, mostly located at the central regions of the protein, are highly protected from hydrogen/deuterium exchange (Fig. 1*A*), which is distinct from the protected amide protons of the native state

* The costs of publication of this article were defrayed in part by the payment of page charges. This article must therefore be hereby marked "*advertisement*" in accordance with 18 U.S.C. Section 1734 solely to indicate this fact.

§ These two authors contributed equally to this work.

** To whom correspondence should be addressed: Institute for Protein Research, Osaka University, Yamadaoka 3-2, Suita, Osaka 565-0871, Japan. Tel.: 81-6-6879-8614; Fax: 81-6-6879-8616; E-mail: ygoto@protein.osaka-u.ac.jp.

[1] The abbreviations used are: β2-m, β_2-microglobulin; C_m, mid-point concentration of guanidine hydrochloride-induced unfolding; ΔG_U, Gibbs free energy change of unfolding; Gdn-HCl, guanidine hydrochloride; ThT, thioflavin T; Pro mutations, proline substitutions of V9P, L23P, L39P, V49P, H51P, L54P, L65P, V82P, and V93P in β2-m; Pro mutants, mutants with a proline substitution; EM, electron microscopy.

This paper is available on line at http://www.jbc.org

Downloaded from http://www.jbc.org/ at OSAKA UNIVERSITY on February 7, 2019

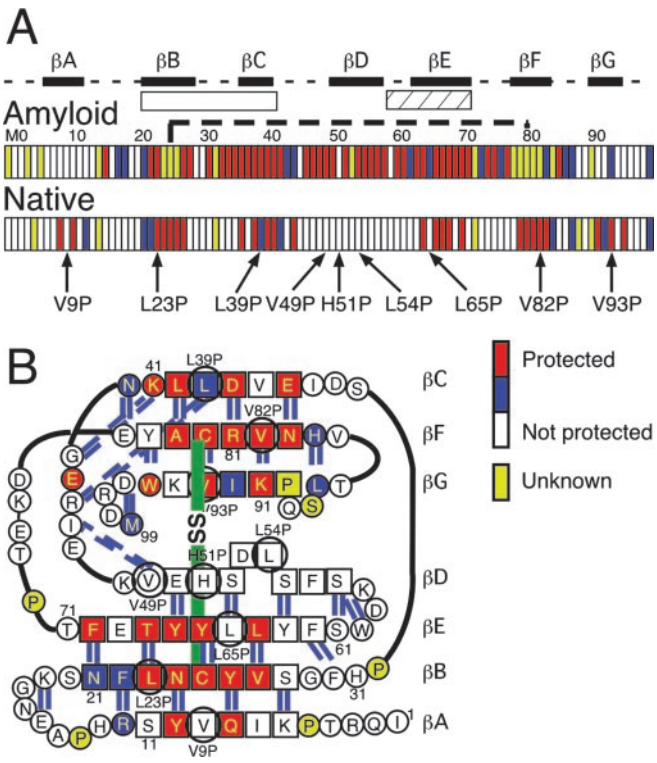

FIG. 1. **Protected residues in the amyloid fibril and the native state of β2-m and the position of Pro-mutations (*A*) and schematic representation of the secondary structure of the native state of β2-m (*B*).** *A*, arrows show the position of Pro mutations. *Filled bars* indicate the position of β-strands found in the native structure. *Open* and *striped boxes* indicate the positions of isolated amyloidogenic peptides, Ser-20–Lys-41 (7) and Asp-59–Thr-71 (5), respectively. The *broken line* depicts the disulfide bond between Cys-25 and Cys-80. *B*, secondary structures in the native state are indicated with amino acid sequences, hydrogen bonds (*broken line*), and the numbering of β-strands. The *large circles* show the position of the mutations. The degree of protection against hydrogen/deuterium exchange in amyloid fibril (22) and native state (25) in each residue was represented by different colors.

protein (Fig. 1) (22). The distribution of preferential proteolytic sites confirmed the protected central regions and the exposed N- and C-terminal regions (23). However, the reduced β2-m, in which the disulfide bond between Cys-25 and Cys-80 (Fig. 1) is reduced, cannot form straight needle-like amyloid fibrils (24), although this molecule has both of these two minimal sequence regions. Instead, the reduced β2-m forms flexible, thin filaments, suggesting that the mature fibril is made of several filaments (20, 25). The recovery of the fibril formation of the K3 peptide (Ser-20–Lys-41) upon removal of the nonessential regions indicates that regions other than the minimal region control fibril formation.

β2-m, at neutral pH, assumes a typical immunoglobulin domain-fold consisting of seven β-strands (Fig. 1*B*) (26–28). To examine the role of each β-strand, we prepared mutants that have a proline (Pro) substitution at the central hydrophobic amino acid, except for the β D strand. Because the β D strand forms the β-bulge, which separates this strand into two parts, we prepared three mutants, V49P, H51P, and L54P. Because Pro is the least favored amino acid at the center of the β-strand (29, 30), each Pro substitution in β2-m (Pro mutation) should affect the formation of amyloid fibrils to a different extent depending on the role of each region. The seed-dependent extension reaction, performed at pH 2.5, is a reproducible and quantitative experiment suitable for characterizing the amyloid fibril formation kinetics of β2-m. However, amyloid fibrils formed at pH 2.5 are unstable at neutral pH, suggesting that additional cellular components are involved in stabilization of the amyloid fibrils *in vivo*. Therefore, nine mutants were examined for their ability to form amyloid fibrils at pH 2.5 by the seed-dependent extension reaction. To further understand the mechanism of the mutational effects, we measured the stability against guanidine hydrochloride (Gdn-HCl) denaturation of the amyloid fibrils at pH 2.5 and the native states at pH 8. Because of the instability of the native state at pH 2.5 (24), the experiments at pH 2.5, although not physiological, can directly extract the effects of mutations on the fibril formation and the stability of amyloid fibrils, separated from the effects on the native state.

EXPERIMENTAL PROCEDURES

Construction of an Expression Plasmid for Wild-type β2-m—For the production of recombinant β2-m, *Pichia pastoris* was used (7, 24). However, this expression system was unsuitable for producing unstable mutants, because the cellular quality control system disallows the release of unstable protein from the secretory pathway (31–33). Because the Pro-mutation may destabilize the native structure of β2-m, and thus, the proteins may not be secreted in the *P. pastoris* expression system, an *Escherichia coli* expression system was selected for producing recombinant β2-m and its mutants. cDNA encoding β2-m was amplified by PCR using *Pfu* Turbo DNA polymerase (Stratagene Cloning Systems, La Jolla, CA). The amplified DNA fragment was cloned into the *E. coli* expression vector pAED4 (34). A Met residue was always present at the N-terminal position of the recombinant protein, which was referred to as M0. Nine Pro mutants, V9P, L23P, L39P, V49P, H51P, L54P, L65P, V82P, and V93P, were prepared using the QuikChange site-directed mutagenesis kit (Stratagene). Fig. 1 shows the distribution of these mutations on the sequence of β2-m.

Expression and Purification of Wild-type β2-m and Pro Mutants—Prepared mutants were expressed in *E. coli* BL21 (DE3) pLysS (Novagen, Inc., Madison, WI). Wild-type and all mutant β2-ms accumulated in inclusion bodies. These inclusion bodies were dissolved in 20 mM Tris-HCl (pH 8.0) containing 8 M urea and air-oxidized for 2–3 days at 4 °C. Formation of the intrachain disulfide bond was confirmed by reverse-phase high performance liquid chromatography (35). After air oxidation, the sample was dialyzed against 20 mM Tris-HCl (pH 8) to refold the proteins. The refolded sample was then subjected to DEAE-Sepharose CL-6B (Amersham Biosciences) equilibrated with 20 mM Tris-HCl (pH 8.0), and the proteins were eluted with a linear concentration gradient of NaCl (0–200 mM). The fraction containing the major peak was dialyzed against deionized water and lyophilized. The lyophilized protein sample was dissolved in 20 mM sodium phosphate buffer (pH 7.5) and applied to a HiPrep 26/60 Sephacryl S-100 high resolution column (Amersham Biosciences) equilibrated with 20 mM sodium phosphate buffer (pH 7.5), and the fraction containing the major peak was collected, dialyzed against deionized water, and lyophilized.

The molecular weight of the purified proteins was measured by matrix-assisted laser desorption ionization time-of-flight mass spectrometry (Applied Biosystems, Foster City, CA) and was correct in each case (±0.025%). Monomer concentrations of wild-type and mutant β2-ms were determined by measuring the UV absorption using a U-3000 spectrophotometer (Hitachi, Tokyo, Japan), at 25 °C. The protein extinction coefficient (ϵ = 19,300 M^{-1} cm^{-1}) was calculated from amino acid sequence data (36).

Fluorometric Analysis of Fibrillogenesis with Thioflavin T—Amyloid fibril formation by wild-type and mutant β2-ms was carried out using the seed-dependent fibril extension method (37–39) in which fragmented fibrils (seeds) are extended with the monomeric proteins at pH 2.5 and 37 °C. The reaction was monitored by fluorometric analysis with thioflavin T (ThT). Native β2-m fibrils were originally purified from Baker's cyst wall excised from the popliteal fossa of a patient suffering from dialysis-related amyloidosis (16). In this study the seed fibrils were prepared by the repeated extension reaction of the seeds previously generated with native β2-m fibrils, and β2-m expressed in *P. pastoris* (7, 24) with monomeric wild-type β2-m that was expressed in *E. coli*.

Briefly, the extension reaction was started by increasing the temperature to 37 °C by placing the samples in an air incubator. From each reaction tube, an aliquot of 7.5 μl was taken and mixed with 1.5 ml of 5 μM ThT in 50 mM glycine-NaOH buffer (pH 8.5), and the fluorescence of ThT was measured using a fluorescence spectrophotometer, F-4500 (Hitachi), at 25 °C with excitation at 445 nm and emission at 485 nm.

Downloaded from http://www.jbc.org/ at OSAKA UNIVERSITY on February 7, 2019

The amyloid extension reactions of mutant β2-m were carried out in a similar manner.

Precipitation Assay for Amyloid Fibrils—After a 4-day incubation with seeds at 37 °C the solutions were centrifuged (15,000 × *g*, 4 °C, 2 h) to precipitate amyloid fibrils. The concentration of proteins in supernatant was determined by UV absorption, and the precipitated fraction was calculated by subtracting this value from the initial concentration of monomeric proteins.

Electron Microscopy—Aliquots (5 μl) of each amyloid extension reaction were diluted with distilled water (95 μl), which was kept at room temperature. These diluted samples were spread on carbon-coated grids, and the solution was allowed to stand for 2–3 min. The excess solution was then removed with filter paper, and the residual solution was allowed to air dry before the grids were negatively stained with 1% phosphotungstic acid (pH 7.0). These samples were examined under an H-7000 electron microscope (Hitachi) with an acceleration voltage of 75 kV.

Circular Dichroism—Circular dichroism (CD) measurements were performed with a J-720 spectropolarimeter (Jasco, Tokyo, Japan). The standard buffers for spectroscopic measurements were 20 mM Tris-HCl (pH 8.0) and 10 mM glycine-HCl (pH 2.5). For far-UV measurement of the amyloid fibrils, 50 mM citrate-NaOH buffer (pH 2.5) containing 100 mM NaCl at an amyloid fibril concentration of 8.5 μM was used. Amyloid fibrils were prepared by the following method. After 4 days of incubation with seeds at 37 °C, protein solutions were centrifuged (15,000 × *g*, 4 °C, 2 h) to precipitate amyloid fibrils. The protein concentration in the supernatant was measured by UV absorption to estimate the amount of fibrils precipitated. Precipitated fibrils were then resuspended in 50 mM citrate-NaOH buffer (pH 2.5) containing 100 mM NaCl, which was used as a stock amyloid fibril solution. The amyloid fibrils for the unfolding experiments were prepared using the same method as above.

Equilibrium Denaturation by Guanidine Hydrochloride—Gdn-HCl-dependent unfolding of wild-type β2-m and Pro mutants in the monomeric and amyloid fibril states were measured using the change in the intrinsic tryptophan fluorescence associated with conformational change. Buffers used for the amyloid fibril and native states were 50 mM citrate-NaOH (pH 2.5) with 100 mM NaCl and 20 mM Tris-HCl (pH 8.0), respectively. Before the measurements, 25–30 samples containing various concentrations of Gdn-HCl were equilibrated at 25 °C for 24 h. Fluorescence spectra were measured with a fluorescence spectrophotometer, F-4500 (Hitachi), at 25 °C with excitation at 295 nm monitored in the range of 300–450 nm at a protein concentration of 0.05 mg·ml^{-1}.

When the transition curves were constructed by plotting the tryptophan fluorescence intensity at a particular wavelength (*e.g.* 350 nm) against the concentration of Gdn-HCl, scattering of the data points was observed, particularly for amyloid fibrils. This scattering, which was probably caused by the fluctuation of protein concentration, demonstrates the difficulty of dealing with aggregation-prone amyloid fibrils. Usually in these cases shift of the maximum emission wavelength or a ratio of intensities at two different emission wavelengths has been used to obtain a smooth transition curve. However, transition curves produced by either of these two methods do not represent the fraction of each structural state. In other words, the midpoint of the transition represented by these two methods does not agree with the true midpoint of the unfolding transition. Instead, a mathematically exact transition curve can be obtained by performing deconvolution of the spectra. Emission spectra were represented by a combination of the spectra of the amyloid (or native) and unfolded states, so that fractions of the two states were obtained at respective concentrations of Gdn-HCl. We used the spectrum acquired without denaturant as the reference amyloid fibril or native state. The spectrum in the presence of 6 M Gdn-HCl was used as a reference spectrum for the unfolded state for each mutant. To obtain the fraction of unfolded species (f_U), the fluorescence spectra from 310 to 450 nm were fitted to the equation $F = \alpha(f_U F_{6\,M} + (1 - f_U)F_{0\,M})$, where F is the spectrum for a sample with each concentration of Gdn-HCl, $F_{0\,M}$ and $F_{6\,M}$, for 0 M and 6 M Gdn-HCl, respectively, f_U is the fractional population of unfolded species, and α is a variable term for fluorescence intensity. f_U was plotted against Gdn-HCl concentration. In the analysis of the unfolding transition of the native state at pH 8, a standard linear relation was assumed between free energy of unfolding (ΔG_U) and denaturant concentration ([Gdn-HCl]); $\Delta G_U = \Delta G_{U,H20} - m$[Gdn-HCl], where $\Delta G_{U,H20}$ is a free energy of unfolding in water and m is the dependence of ΔG_U on Gdn-HCl concentration.

RESULTS

Amyloid Fibril Formation Monitored by ThT Fluorescence—To analyze the effects of Pro mutations on the amyloidogenic potential, the seed-dependent amyloid fibril extensions of wild-type and mutant β2-ms were examined with wild-type seeds. When monitored by ThT fluorescence, the extension reactions of wild-type β2-m at pH 2.5, completed in 2 h, were consistent with previous reports (19, 24) (Fig. 2*A*). The kinetics of fibril extension was affected to varying degrees by the mutations, and significant retardation of the extension reaction was observed for several mutants (*i.e.* L23P, L39P, H51P, L65P, and V82P). Comparison of all the mutants and wild-type β2-ms is summarized in Figs. 2*B* and 3*A*. In addition, after 4 days of incubation, all samples were centrifuged at 15,000 × *g*, and the amounts of precipitated fibrils were estimated (Figs. 2*C* and 3*B*). With the exception of L65P, the data from the two different assays were qualitatively consistent (compare Figs. 2*B* and 2*C* or Figs. 3, *A* and *B*).

These experiments revealed that the introduction of Pro into the different native β-strands affected amyloid fibril formation to various extents. After 4 days of incubation, L23P and V82P showed less than 30% of the ThT fluorescence and precipitated fractions in comparison with those of wild-type β2-m, indicating decreased tendencies toward amyloid fibril formation. These two mutations were introduced into the β B and F strands, which are connected by the intrachain S-S bond (Fig. 1). Among the mutants with a substitution in the β D strand, H51P also exhibited about 40% of amyloid fibril formation at 4 days compared with wild type. However, we did not observe the marked decreases in ThT fluorescence and precipitated fraction for V49P and L54P, which are also in the β D strand. The intensity of ThT fluorescence for V49P was about twice that of wild-type β2-m. This could be explained by the increased sensitivity of ThT to the fibrils of V49P mutant (see below).

For V9P and V93P, ThT fluorescence and the amount of precipitated proteins were almost identical to those of the wild-type protein, indicating little effect of these mutations on fibril formation. Although L65P showed very little ThT fluorescence, more than 90% of protein was precipitated by the centrifugation at 15,000 × *g*. The precipitated fraction of this mutant exhibited a far-UV spectrum typical of amyloid fibrils and similar to amyloid fibrils of the wild-type protein (see below). In addition, the stability of fibrils formed by this mutant was identical to that of wild-type β2-m (see below). Thus, we believe that a considerable amount of fibrils was formed with L65P. L65P may alter the interactions between fibrils and ThT, resulting in a large decrease in fluorescence intensity.

These results imply that, when compared with different proteins, the intensity of ThT fluorescence is not always proportional to the amount of amyloid fibrils. In our previous paper (7) we proposed that the ThT fluorescence can change depending on the morphology of amyloid fibrils. Although the fresh amyloid fibrils without lateral aggregation between fibrils show a high fluorescence intensity, further incubation decreases ThT fluorescence, probably due to the lateral aggregation expelling ThT bound between fibrils. We noticed that there were more lateral aggregates in fibrils of L65P and H51P, as determined by electron microscopy (EM), than in fibrils of other mutants and wild-type protein (see below). H51P also showed a smaller ThT fluorescence than that expected from the precipitated fraction. On the other hand EM images of fibrils made of V49P showed no distinct feature responsible for the marked ThT fluorescence (see below). Although the exact mechanism is not clear, it is likely that the difference in high order structure of amyloid fibrils results in the observed difference in ThT fluorescence.

Amyloid Fibrils Observed by Electron Microscopy and Circular Dichroism—The EM images of the mutants were measured after a few days of the fibril extension reaction (Fig. 4). Inter-

Downloaded from http://www.jbc.org/ at OSAKA UNIVERSITY on February 7, 2019

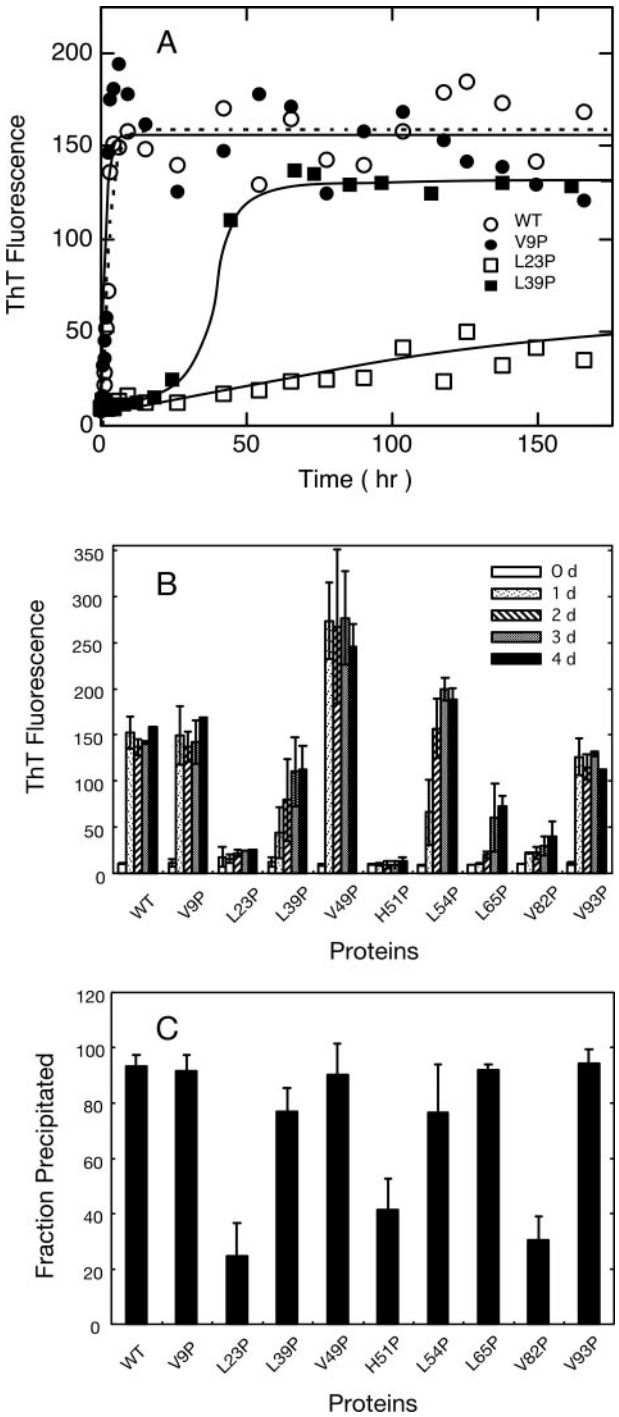

FIG. 2. **Formation of amyloid fibrils detected by ThT fluorescence (*A* and *B*) and the quantification of precipitated proteins after 4 days of incubation (*C*).** The mutants and wild-type (*WT*) β2-ms (25 μM) were incubated with seeds of wild-type β2-m (5 μM) at pH 2.5 and 37 °C in the buffer of 50 mM citrate-NaOH and 100 mM NaCl. *d*, day. *A*, as a representative example, kinetics of amyloid fibril formation of wild-type (○: *broken line*), V9P (●), L23P (□), and L39P (■) were shown in this *panel*. *B*, ThT fluorescence at starting point (*open bar*), after 1 day (*dotted bar*), after 2 days (*striped*), after 3 days (*gray*), and after 4 days (*filled*) of incubation with seed. For all mutant and wild-type proteins, the measurements were carried out twice. *C*, the amount of precipitated protein was estimated after 4 days of incubation with seed. For V49P and L54P, the experiments were repeated twice. For other mutants and wild-type β2-m, the measurements were repeated four times.

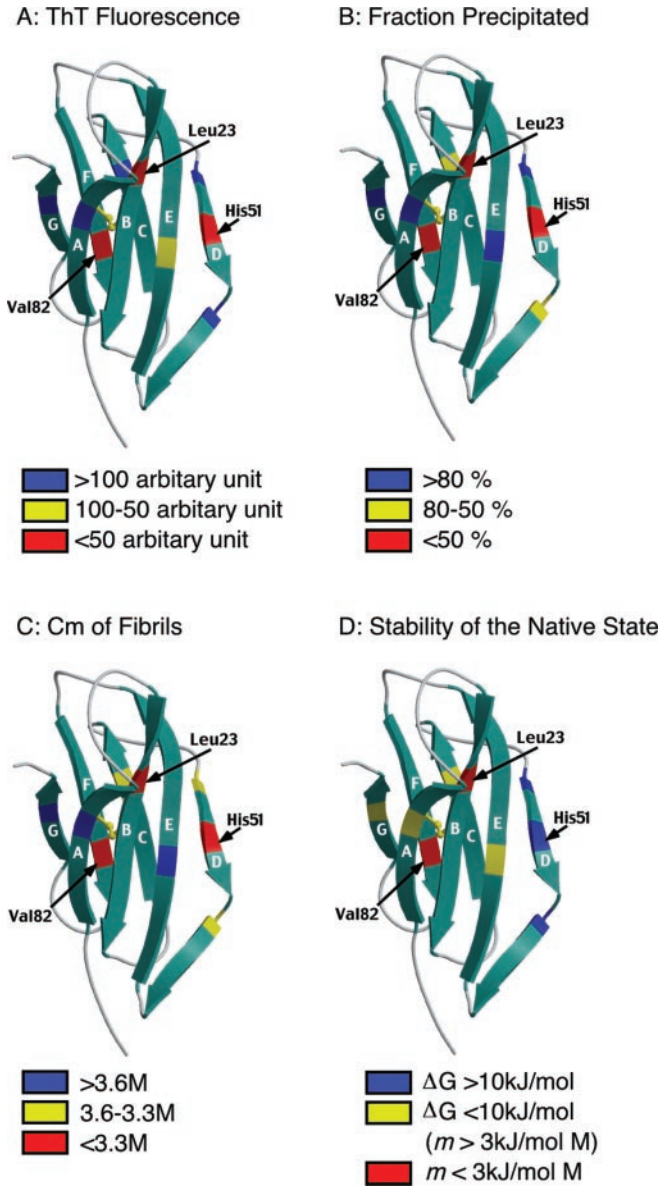

FIG. 3. **The effects of Pro mutations on the amyloidogenicity and folding of β2-m mapped on its native structure.** The fibril formations after 4 days of incubation detected by ThT fluorescence (*A*) and precipitation assay (*B*). The stabilities of amyloid fibrils (*C*) and the native state (*D*) probed by the Gdn-HCl-induced unfolding are shown. The three-dimensional structure of β2-m (PDB entry 1QQD) was drawn using MOLSCRIPT (47).

estingly, we observed straight needle-like amyloid fibrils for all the samples examined. For all mutant β2-ms, the newly formed straight fibrils, with a diameter of about 10–15 nm and a longitudinal periodicity, were similar to the wild-type β2-m amyloid fibrils (19, 24). However, we observed the lateral aggregates of fibrils more frequently in H51P and L65P than in the others. Because L23P, H51P, and V82P showed very small ThT fluorescence, we first expected that ThT fluorescence and precipitates of these mutants arise from the amorphous aggregates. In fact even these mutants formed straight and rigid fibrils. The amount of fibrils of these mutants seemed to be less than that of wild-type β2-m, although EM is only a qualitative method to estimate the amounts.

To further confirm the formation of amyloid fibrils for the Pro mutants, we measured the CD spectra of the precipitated fractions by centrifugation (15,000 × *g*) after 4 days of incubation with wild-type seeds at pH 2.5 (Fig. 5*A*). As a control we measured the CD spectra of the monomeric states of the mutants at pH 2.5 (Fig. 5*B*). Resuspended amyloid fibrils in the acidic buffer showed a far-UV CD spectra similar to that of

Downloaded from http://www.jbc.org/ at OSAKA UNIVERSITY on February 7, 2019

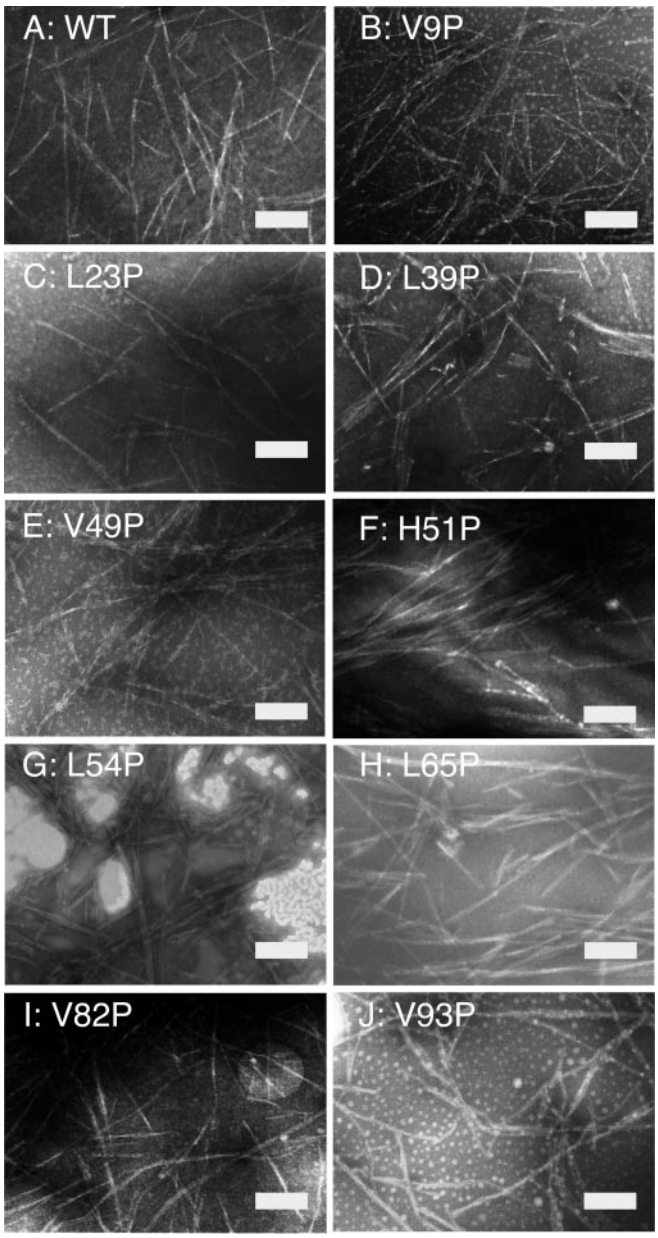

FIG. 4. **Electron micrographs of amyloid fibrils of Pro mutants.** Amyloid fibrils were formed by incubation with wild-type seeds at 37 °C in a buffer of 50 mM citrate-NaOH and 100 mM NaCl (pH 2.5). Wild-type, V9P, and V93P β2-ms were incubated for 4 h before measurement. L23P, H51P, and V82P were incubated for 5 days before measurement. L39P, V49P, L54P, and L65P were incubated for 2 days before measurement. *A*, wild-type (*WT*); *B*, V9P; *C*, L23P; *D*, L39P; *E*, V49P; *F*, H51P; *G*, L54P; *H*, L65P; *I*, V82P; *J*, V93P. The *bars* indicate a length of 200 nm.

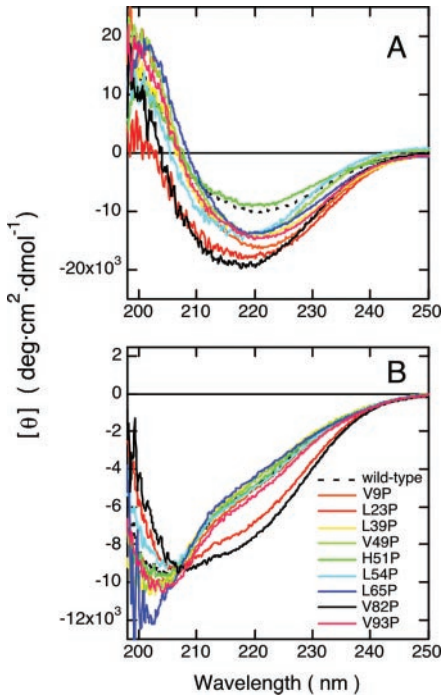

FIG. 5. **Far-UV CD spectra of amyloid fibril (*A*) and acid-denatured (*B*) states of Pro mutants at pH 2.5.** CD spectra were measured using a 1-mm cell at the protein concentration of 8.5 μM as a monomer in the buffer of 50 mM citrate-NaOH and 100 mM NaCl (pH 2.5) at 25 °C. Amyloid fibrils were collected by centrifugation (15,000 × *g*, 4 °C, 2 h) and resuspended in buffer.

wild-type β2-m fibrils (Fig. 5*A*). The intensity of the negative varied slightly, partly due to the difficulty in achieving a homogeneous suspension. Except for L23P and V82P, spectra of all mutants had a minimum around 220 nm, which is typical for β2-m amyloid fibrils, confirming the formation of amyloid fibrils with these mutants. Spectra of L23P and V82P fibrils showed a slight shift in the minimum to a shorter wavelength (*i.e.* 218 nm) compared with other mutants and wild-type β2-ms. These results suggest that amyloid fibrils of L23P and V82P assume a slightly different structure from that of wild-type β2-m amyloid fibrils.

It is intriguing that the monomeric acid-denatured states of L23P and V82P showed CD spectra different from other mutants and wild-type β2-ms (Fig. 5*B*). The negative intensity at 222 nm of these two mutants was larger than for other species, suggesting a small but notable amount of α-helical content in the acid-denatured L23P and V82P. Other mutants gave almost identical spectra to that of the wild-type protein, indicating these mutants shared a substantially unfolded structure similar to wild-type protein in the acid-denatured state. Therefore, it is likely that the higher α-helical preference of the acid-denatured states of L23P and V82P is related to the suppressed fibril formation of these mutants.

Stabilities of the Amyloid Fibrils and Native States—We measured the stability of amyloid fibrils and native states of the Pro mutants to identify the origin of the distinctive effects of each mutation on fibril formation. Amyloid fibrils of mutants were prepared by a 4 days of incubation with seeds. The fibrils were separated from the monomers by centrifugation and subsequently resuspended homogeneously into the pH 2.5 buffer. Gdn-HCl-induced unfolding transitions of these samples at pH 2.5 were measured using tryptophan fluorescence, which illustrates the difference between fibril and monomeric unfolded states (Fig. 6). The tryptophan fluorescence of amyloid fibrils for the wild-type β2-m showed a maximum at 340 nm (data not shown). The addition of Gdn-HCl resulted in a red shift of the maximal wavelength to 350 nm, with an accompanying decrease in the maximal intensity, showing that the amyloid fibrils were depolymerized into the unfolded monomers. The amyloid fibrils of the Pro mutants also showed similar spectral changes, although the spectra of the fibrils varied slightly depending on the mutants. The fraction of the monomeric unfolded state was calculated by fitting the spectrum at a given denaturant concentration to a combined spectrum of fibril and unfolded states. The midpoint concentrations of Gdn-HCl-induced unfolding (C_m) are summarized in Table I. Because the exact mechanism for the unfolding of amyloid fibrils by Gdn-HCl is unknown, we did not carry out any further analysis in this study.

The Gdn-HCl-dependent transitions between the native and

Downloaded from http://www.jbc.org/ at OSAKA UNIVERSITY on February 7, 2019

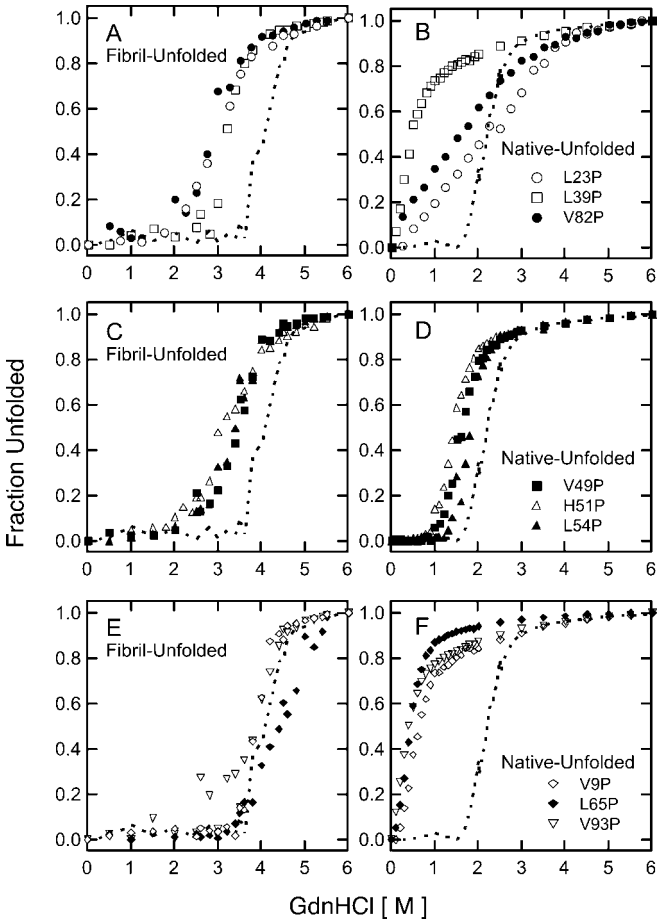

FIG. 6. **Gdn-HCl-induced unfolding transitions of amyloid fibrils at pH 2.5 (*A*, *C*, and *E*) and the native structures at pH 8.0 (*B*, *D*, and *F*) of Pro mutants.** Amyloid fibrils were collected by centrifugation (15,000 × *g*, 4 °C, 2 h) and resuspended to the buffer. Unfolding was monitored by following the changes in tryptophan fluorescence spectra. As a reference, the transition curves of the fibril (*A*, *C*, and *E*) and native states (*B*, *D*, and *F*) of wild-type β2-m were shown as a *broken line* in each *panel*. *A* and *B*, the unfolding transition of L23P (○), L39P (□), and V82P (●) are shown. *C* and *D*, the unfolding transition of V49P (■), H51P (△), and L54P (▲) are shown. *E* and *F*, the unfolding transition of V9P (◇), L65P (◆), and V93P (▽) are shown.

TABLE I
The stability of the amyloid fibril and the native state of wild-type and nine Pro-mutants of β2-m

Protein	Amyloid fibril at pH 2.5 (C_m)	Native State at pH 8.0	
		ΔG in H_2O	m
	M	$kJ \cdot mol^{-1}$	$kJ \cdot mol^{-1} M^{-1}$
Wild type	4.1	22.0 ± 1.1	10.0 ± 0.5
V9P	3.9	6.4 ± 0.3	9.4 ± 0.8
L23P	3.0	6.1 ± 0.3	2.8 ± 0.1
L39P	3.3	5.3 ± 0.6	9.9 ± 1.2
V49P	3.4	15.8 ± 1.0	9.6 ± 0.6
H51P	3.2	13.7 ± 0.9	9.3 ± 0.6
L54P	3.3	19.7 ± 2.0	10.7 ± 1.1
L65P	4.4	5.2 ± 0.6	10.8 ± 1.1
V82P	2.9	4.5 ± 0.1	2.8 ± 0.1
V93P	3.8	4.7 ± 0.5	10.5 ± 1.2

unfolded states at pH 8 were also measured using the difference of tryptophan fluorescence spectra between these two states (Fig. 6, *B*, *D*, and *F*). The native state of wild-type β2-m had a maximum at 338 nm, slightly shorter than that of the amyloid fibrils (data not shown). Both of the tryptophan residues of β2-m in the native state (Trp-60 on the β-turn connecting β-strand D and E and Trp-95 on the C-terminal end of β-strand D) are largely exposed to the solvent (Fig. 1*B*). Comparison of the maximal wavelength for the native state (338 nm) and the amyloid fibrils (340 nm) suggests that the tryptophan residues of the amyloid fibrils are more exposed than those of the native state. The unfolding of the native state of wild-type β2-m was accompanied by a red shift of the maximal wavelength to 350 nm and a decrease in the fluorescence intensity. The mutants showed similar changes in spectra. For the unfolding of the native states, we estimated the free energy change of unfolding in the absence of denaturant based on a two-state folding mechanism and linear relation between free energy and denaturant concentration (Table I).

Because the data were obtained at different pH values (*i.e.* pH 2.5 for amyloid fibril and pH 8 for native state), it is important to consider the effects of the difference in pH. Moreover, we used two different buffer systems, *i.e.* citrate-NaOH at pH 2.5 for amyloid fibrils and Tris-HCl at pH 8.0 for the native state. In our case Pro was substituted for hydrophobic amino acids, except for H51P. Substitution of Pro for the hydrophobic amino acids would change the hydrogen-bond, hydrophobic interactions, and the conformational entropy. In general, these interactions are relatively insensitive to the pH change and buffer components. Therefore, we assumed that the pH effects (*i.e.* superimposing acid-unfolding effects) contribute to the stability of all the mutants, except H51P, to a similar extent. For the H51P mutant, the mutation loses one positive charge at pH 2.5, whereas the net charge does not change at pH 8.0. Contrary to the expectation that the decrease in net charge stabilizes the amyloid fibrils of β2-m at pH 2.5, the H51P mutation caused destabilization of the amyloid fibrils. This indicates that change in the net charge does not explain the variation in stability of amyloid fibrils among β2-m mutants.

Comparison of the unfolding transition curves of the native and amyloid states showed that the mutations can be classified into three types in terms of their effects. The first type of mutation shows significant destabilization of both the native and amyloid states. L23P and V82P with mutations in the β-strands connected by an intrachain disulfide bond had the lowest tendencies to form amyloid fibrils. The stability of amyloid fibrils and native states of these two mutants was lower than those of the wild-type protein (Fig. 6, *A* and *B*, and Table I). Entirely different unfolding curves with decreased m values were observed for the native states of L23P and V82P (Fig. 6*B* and Table I). The m value correlates strongly with the change of accessible surface area between the native and unfolded states (40), and thus, the native structures of L23P and V82P at pH 8 are likely to be more disordered than those of other mutants and wild-type proteins. Far-UV CD spectra of these mutants in the native state were distinct from wild-type β2-m, although other mutants displayed almost identical spectra to that of the wild-type (data not shown). These indicate that the native structures of L23P and V82P were partly destroyed before the addition of Gdn-HCl. In addition, L39P showed a marked decrease in stability of both the amyloid fibrils and native states. However, the unfolding transition from the native state of this mutant showed an m value close to that of the wild-type protein (Fig. 6*B* and Table I).

The mutations in the β D strand (V49P, H51P, and L54P) again exhibited a destabilizing effect on both the native and amyloid fibril states. The mutations that constitute this group destabilized amyloid fibrils significantly, although slightly less than the first type of mutations. On the other hand, the decreases in stability of the native states were minimal among the mutants (Fig. 6, *C* and *D*, and Table I). Previous NMR studies (22, 25, 41) reported that in the native state residues in the β-strands, except the β D strand, were strongly protected from hydrogen/deuterium exchange, indicating the presence of

Downloaded from http://www.jbc.org/ at OSAKA UNIVERSITY on February 7, 2019

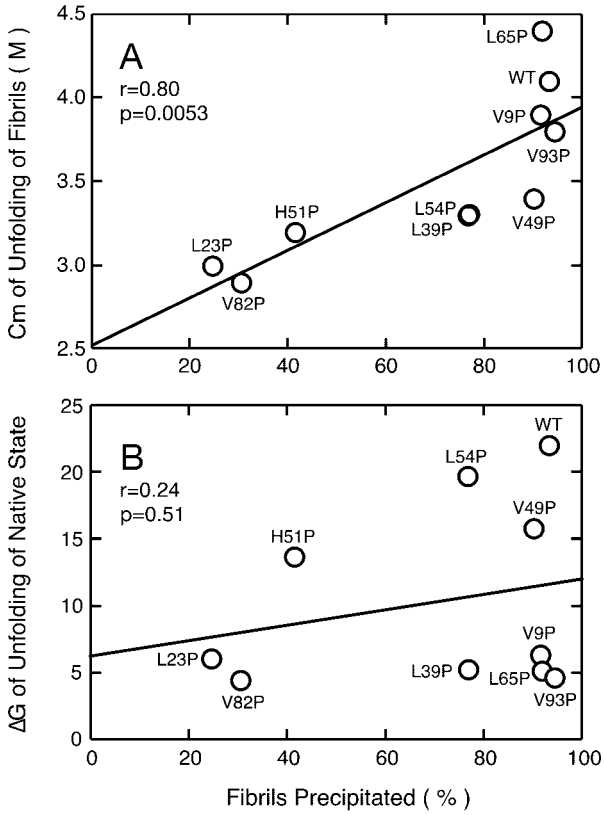

FIG. 7. **The correlation of the stability of amyloid fibril (*A*) and native state (*B*) with amyloidogenic potential.** The data from the precipitation assay for this plot represents the amyloidogenic potential. The values of *r* and *p* indicate linear correlation coefficient and probability, respectively. *WT*, wild type.

an extensive stable core consisting of all the β-strands, except β D (Fig. 1). β D connects the two β-sheet layers and is not involved in the core of the native structure. On the other hand the β D strand constitutes the core of amyloid fibrils (Fig. 1*A*). Thus, mutations in the β D strand did not significantly affect the stability of the native state of β2-m, whereas they notably destabilized the amyloid fibrils (Fig. 3, *C* and *D*).

The third type of mutation, V9P, L65P, and V93P, significantly destabilized only the native state. In contrast to the mutations in β D strand, these mutations showed a marked decrease in the stability of the native state (Fig. 6*F*). Intriguingly, there was little effect on the stability of amyloid fibrils (Fig. 6*E*). Val-9 and Val-93 are included in the terminal β A and β G strands, which do not participate in the amyloid fibrils (Fig. 1*A*) (22, 23), and thus, the mutations in these strands do not affect the stability of the amyloid fibrils. Leu-65 was thought to be buried inside of the amyloid fibrils. Therefore, it is unclear why amyloid fibrils of L65P exhibited a stability similar to that of the wild-type β2-m.

DISCUSSION

Correlation between Amyloidogenicity and Stability of Amyloid Fibrils—A large decrease in amyloidogenicity was observed in L23P, H51P, and V82P, which exist in different native β-strands. To identify the origin of the effects of each mutation on fibril formation, we measured the stability of amyloid fibrils and native states of Pro mutants. The effects of these mutations were distinct between the native states and amyloid fibrils. To clarify the effects of the altered stability of the native and amyloid states, we plotted the stability parameters against amyloidogenicity represented by the fraction of fibrils precipitated (Fig. 7). The correlation coefficient and probability of the stability of amyloid and the amyloidogenicity were 0.80 and 0.0053, respectively (Fig. 7*A*), indicating that the stability of amyloid fibrils significantly correlates with the amyloidogenic potential. The correlation coefficient and probability of the native state and amyloidogenicity were 0.24 and 0.51, respectively (Fig. 7*B*). These values indicate that the correlation between the stability of the native states and amyloidogenic potential is very weak or negligible. In other words, the destabilization of the amyloid fibrils is one of the key factors responsible for the reduction of amyloidogenic potential. The results indicate that the regions including β B, β D, and β F strands directly determine the amyloidogenic potential of β2-m by controlling the stability of amyloid fibrils.

The Role of the Nonessential Regions—The β2-m molecule is assumed to consist of two regions, minimal (or essential) and nonessential regions for amyloid fibril formation (7). The minimal region even after isolation can form fibrils by itself and may constitute the core of the amyloid fibrils. Amyloidogenic peptides (Ser-20–Lys-41 and Asp-59–Thr-71, see *boxes* in Fig. 1*A*) accommodate such regions (5, 7). One of these minimal peptides (Ser-20–Lys-41) includes Leu-23, and substitution of this amino acid with Pro predominantly decreased amyloidogenicity. However, we also found that mutations such as H51P and V82P, belonging to the nonessential region, significantly decreased the amyloidogenic potential. This demonstrates the important role of nonessential regions in controlling the amyloidogenicity of proteins. The nonessential regions not only participate in fibrillogenesis but also determine the amyloidogenic potential of the full-length protein. One mechanism raised in this study is that the nonessential regions contribute to increasing the overall stability of amyloid fibrils, consequently increasing the amyloidogenicity.

Leu-23 and Val-82 are on the β B and β F strands, respectively, in the native structure of β2-m. β B and β F strands are connected by an intrachain disulfide bond between Cys-25 and Cys-80, which is critical for the formation of amyloid fibrils (24, 35). Helical propensity located at Lys-58–Thr-68 was suggested to play an inhibitory role in fibril formation of β2-m (25). Interestingly, the monomeric acid-denatured state of reduced β2-m exhibited a far-UV spectrum with slightly larger negative ellipticity around 222 nm than that of oxidized protein (24), suggesting an increase of helical content in reduced β2-m. In the far-UV spectra of the acid-denatured state of L23P and V82P, negative ellipticities larger than that of wild-type were also observed (Fig. 5*B*). Therefore, in addition to the effects on the stability of amyloid fibrils, it is possible that mutations around the disulfide bond increase the helical propensity of the acid-unfolded state, an amyloidogenic intermediate, thus decreasing the amyloidogenic potential.

His51 is located on the β D strand, which is important for amyloid fibril formation (27). The β D strand is the edge strand that does not have a partner to form a hydrogen bond (Fig. 1*C*) and could be inherently aggregation prone (42). It is assumed that conformational change of the side chain of His-51 removes its protective feature of charge repulsion in the monomeric β2-m against aggregation, thus allowing amyloid fibril formation (27). Because Pro is supposed to inhibit the interaction between edge strands, our result showing that H51P was less amyloidogenic than wild-type is consistent with the proposed role of His-51. However, V49P and L54P exhibited only minor effects on amyloid formation. Therefore, the overall role of the β D strand for fibrillogenesis remains unclear.

Determinants of Amyloidogenicity—The conclusion that amyloidogenicity is correlated with stability of the amyloid fibrils rather than that of the native state is partly explained by our unique experimental system for amyloid fibril extension at

Downloaded from http://www.jbc.org/ at OSAKA UNIVERSITY on February 7, 2019

pH 2.5. There is no doubt that the stability and unfolding rate of the native state are the most important factors determining amyloidogenicity of proteins under the physiological conditions, as clearly evidenced with various proteins (8–13). In our experiments performed at pH 2.5, most of the β2-m molecules were acid-denatured, and the effects of Pro-mutations on the native structure could be ignored. This unique experimental system can focus on the role of the denatured state by examining the conformational preference, as shown previously by NMR (25). The present study indicated that the stability of the amyloid fibrils is an additional factor determining the amyloidogenicity of β2-m. Moreover, the small but notable helical preference of L23P and V82P in the acid-denatured state was suggested to play a suppressive role on amyloid fibril formation.

However, there was a deviation from the linear relation between the stability of amyloid fibrils and amyloidogenic potential in L39P, V49P, and L54P. Although these mutants showed decreased stability of the amyloid fibrils (Fig. 6 and Table I), they exhibited a higher propensity to form amyloid fibrils similar to the wild-type protein (Fig. 2). This suggests the participation of additional factors in the formation of amyloid fibrils. Some Pro mutations not only shift the equilibrium but may also alter the kinetics of amyloid fibril formation. Indeed, we observed deceleration of fibril formation in L39P and L54P with a lag phase (Fig. 2, *A* and *B*), although they finally formed similar amounts of amyloid fibrils to the wild-type protein after 4 days of incubation. These mutants showed a decreased stability of the amyloid fibrils compared with that of the wild type. Further experiments were required to clarify the effects of the Pro-mutation on the detailed kinetics of fibril formation.

Mutational analysis of amyloidogenic or aggregation-prone proteins revealed various factors responsible for the formation of amyloid fibrils and aggregation. Chiti *et al.* (14, 15) studied the effects of many mutations of acylphosphatase on the aggregation of this protein. They identified three factors important for the aggregation: hydrophobicity, β-sheet propensity, and net charge of the sequence. Although these factors were found with the aggregates but not with distinct amyloid fibrils, it is likely that these factors also contribute to the amyloid fibril formation of β2-m mutants. Amino acid substitution with Pro critically decreases the β-sheet propensity (29, 30); thus, the small amyloidogenic potentials of L23P, H51P, and V82P were consistent with the reduction of β-sheet propensity.

Implication for the Role of Proline Mutants on Familial Amyloidosis—Several mutations with Pro substituted by other amino acids or mutations in which Pro is newly introduced are found in several types of familial amyloidosis (11, 43–46). The substitution of a certain amino acid (Xaa) with Pro is assumed to cause serious perturbation of the structure of native and/or intermediate states and increases the amyloidogenicity of these mutants (11). However, little is known about the mechanism for the pathogenesis of amyloidosis caused by replacing Pro (from Pro to Xaa). In the present study we found that mutations to Pro, such as L23P, H51P, and V82P, largely decrease the stability of fibrils and consequently their amyloidogenic potential. This suggests that replacing Pro with other amino acids might recover the otherwise suppressed amyloidogenicity. In proteins that are essentially non-amyloidogenic with wild-type sequences, some Pro residues may inhibit the formation of amyloid fibrils by reducing their stability. Thus, removing these Pro residues could increase the stability of fibrils, resulting in familial amyloidosis.

Conclusion—Amyloidogenicity of proteins is determined by a combination of factors. Because the structure of amyloid fibrils is substantially different from those of the native state of the precursor proteins, destabilization or unfolding of the native state is required for amyloid fibrils to form. Therefore, mutations or change of solvent conditions (*e.g.* decrease of pH), destabilizing the native states or increasing the unfolding rate, often trigger the formation of amyloid fibrils. Although detailed structures of the amyloidogenic intermediates are unknown, there is no doubt that the conformational preferences of the denatured state (*e.g.* net charge, hydrophobicity, β-sheet propensity) are important for determining the amyloidogenicity of the proteins. The present study, focusing on the process of fibril formation from the acid-unfolded state with a variety of Pro mutants, revealed that the stability of amyloid fibrils is an additional important factor determining the amyloidogenic potential of the proteins.

Acknowledgments—We thank S. Tsutsumi and M. Kihara for EM measurements and Professor S. Aimoto and Dr. T. Kawakami at the Institute for Protein Research, Osaka University, Osaka, Japan, for the mass spectrometry measurements.

REFERENCES

1. Kelly, J. W. (1996) *Curr. Opin. Struct. Biol.* **6,** 11–17
2. Kelly, J. W. (1998) *Curr. Opin. Struct. Biol.* **8,** 101–106
3. Sigurdsson, E. M., Wisniewski, T., and Frangione, B. (2002) *Trends Mol. Med.* **8,** 411–413
4. Selvaggini, C., De Gioia, L., Cantu, L., Ghibaudi, E., Diomede, L., Passerini, F., Forloni, G., Bugiani, O., Tagliavini, F., and Salmona, M. (1993) *Biochem. Biophys. Res. Commun.* **194,** 1380–1386
5. Jones, S., Manning, J., Kad, N. M., and Radford, S. E. (2003) *J. Mol. Biol.* **325,** 249–257
6. Gustavsson, A., Engström, U., and Westermark, P. (1991) *Biochem. Biophys. Res. Commun.* **175,** 1159–1164
7. Kozhukh, G. V., Hagihara, Y., Kawakami, T., Hasegawa, K., Naiki, H., and Goto, Y. (2002) *J. Biol. Chem.* **277,** 1310–1315
8. Booth, D. R., Sunde, M., Bellotti, V., Robinson, C. V., Hutchinson, W. L., Fraser, P. E., Hawkins, P. N., Dobson, C. M., Radford, S. E., Blake, C. C. F., and Pepys, M. B. (1997) *Nature* **385,** 787–793
9. Souillac, P. O., Uversky, V. N., Millett, I. S., Khurana, R., Doniach, S., and Fink, A. L. (2002) *J. Biol. Chem.* **277,** 12657–12665
10. McCutchen, S. L., Lai, Z. H., Miroy, G. J., Kelly, J. W., and Colon, W. (1995) *Biochemistry* **34,** 13527–13536
11. McCutchen, S. L., Colon, W., and Kelly, J. W. (1993) *Biochemistry* **32,** 12119–12127
12. Hurle, M. R., Helms, L. R., Li, L., Chan, W. N., and Wetzel, R. (1994) *Proc. Natl. Acad. Sci. U. S. A.* **91,** 5446–5450
13. Hammarström, P., Jiang, X., Hurshman, A. R., Powers, E. T., and Kelly, J. W. (2002) *Proc. Natl. Acad. Sci. U. S. A.* **99,** 16427–16432
14. Chiti, F., Calamai, M., Taddei, N., Stefani, M., Ramponi, G., and Dobson, C. M. (2002) *Proc. Natl. Acad. Sci. U. S. A.* **99,** 16419–16426
15. Chiti, F., Taddei, N., Baroni, F., Capanni, C., Stefani, M., Ramponi, G., and Dobson, C. M. (2002) *Nat. Struct. Biol.* **9,** 137–143
16. Gejyo, F., Yamada, T., Odani, S., Nakagawa, Y., Arakawa, M., Kunitomo, T., Kataoka, H., Suzuki, M., Hirasawa, Y., Shirahama, T., Cohen, A. S., and Schmid, K. (1985) *Biochem. Biophys. Res. Commun.* **129,** 701–706
17. Casey, T. T., Stone, W. J., DiRaimondo, C. R., Brantley, B. D., DiRaimondo, C. V., Gorevic, P. D., and Page, D. L. (1986) *Hum. Pathol.* **17,** 731–738
18. Koch, K. M. (1992) *Kidney Int.* **41,** 1416–1429
19. Naiki, H., Hashimoto, N., Suzuki, S., Kimura, H., Nakakuki, K., and Gejyo, F. (1997) *Amyloid* **4,** 223–232
20. Kad, N. M., Myers, S. L., Smith, D. P., Alastair Smith, D., Radford, S. E., and Thomson, N. H. (2003) *J. Mol. Biol.* **330,** 785–797
21. Hasegawa, K., Ohhashi, Y., Yamaguchi, I., Takahashi, N., Tsutsumi, S., Goto, Y., Gejyo, F., and Naiki, H. (2003) *Biochem. Biophys. Res. Commun.* **304,** 101–106
22. Hoshino, M., Katou, H., Hagihara, Y., Hasegawa, K., Naiki, H., and Goto, Y. (2002) *Nat. Struct. Biol.* **9,** 332–336
23. Monti, M., Principe, S., Giorgetti, S., Mangione, P., Merlini, G., Clark, A., Bellotti, V., Amoresano, A., and Pucci, P. (2002) *Protein Sci.* **11,** 2362–2369
24. Ohhashi, Y., Hagihara, Y., Kozhukh, G., Hoshino, M., Hasegawa, K., Yamaguchi, I., Naiki, H., and Goto, Y. (2002) *J. Biochem.* (*Tokyo*) **131,** 45–52
25. Katou, H., Kanno, T., Hoshino, M., Hagihara, Y., Tanaka, H., Kawai, T., Hasegawa, K., Naiki, H., and Goto, Y. (2002) *Protein Sci.* **11,** 2218–2229
26. Bjorkman, P. J., Saper, M. A., Samraoui, B., Bennett, W. S., Strominger, J. L., and Wiley, D. C. (1987) *Nature* **329,** 506–512
27. Trinh, C. H., Smith, D. P., Kalverda, A. P., Phillips, S. E., and Radford, S. E. (2002) *Proc. Natl. Acad. Sci. U. S. A.* **99,** 9771–9776
28. Verdone, G., Corazza, A., Viglino, P., Pettirossi, F., Giorgetti, S., Mangione, P., Andreola, A., Stoppini, M., Bellotti, V., and Esposito, G. (2002) *Protein Sci.* **11,** 487–499
29. Minor, D. L., Jr., and Kim, P. S. (1994) *Nature* **371,** 264–267
30. Minor, D. L., Jr., and Kim, P. S. (1994) *Nature* **367,** 660–663
31. Hagihara, Y., Shiraki, K., Nakamura, T., Uegaki, K., Takagi, M., Imanaka, T., and Yumoto, N. (2002) *J. Biol. Chem.* **277,** 51043–51048
32. Hagihara, Y., and Kim, P. S. (2002) *Proc. Natl. Acad. Sci. U. S. A.* **99,**

Downloaded from http://www.jbc.org/ at OSAKA UNIVERSITY on February 7, 2019

6619–6624
33. Ellgaard, L., Molinari, M., and Helenius, A. (1999) *Science* **286,** 1882–1888
34. Doering, D. S., and Matsudaira, P. (1996) *Biochemistry* **35,** 12677–12685
35. Hong, D. P., Gozu, M., Hasegawa, K., Naiki, H., and Goto, Y. (2002) *J. Biol. Chem.* **277,** 21554–21560
36. Gill, S. C., and von Hippel, P. H. (1989) *Anal. Biochem.* **182,** 319–326
37. Naiki, H., Higuchi, K., Hosokawa, M., and Takeda, T. (1989) *Anal. Biochem.* **177,** 244–249
38. Naiki, H., Higuchi, K., Nakakuki, K., and Takeda, T. (1991) *Lab. Invest.* **65,** 104–110
39. Naiki, H., and Nakakuki, K. (1996) *Lab. Invest.* **74,** 374–383
40. Myers, J. K., Pace, C. N., and Scholtz, J. M. (1995) *Protein Sci.* **4,** 2138–2148
41. McParland, V. J., Kalverda, A. P., Homans, S. W., and Radford, S. E. (2002) *Nat. Struct. Biol.* **9,** 326–331
42. Richardson, J. S., and Richardson, D. C. (2002) *Proc. Natl. Acad. Sci. U. S. A.* **99,** 2754–2759
43. Doh-ura, K., Tateishi, J., Sasaki, H., Kitamoto, T., and Sakaki, Y. (1989) *Biochem. Biophys. Res. Commun.* **163,** 974–979
44. Yamada, M., Itoh, Y., Inaba, A., Wada, Y., Takashima, M., Satoh, S., Kamata, T., Okeda, R., Kayano, T., Suematsu, N., Kitamoto, T., Otomo, E., Matsushita, M., and Mizusawa, H. (1999) *Neurology* **53,** 181–188
45. Brett, M., Persey, M. R., Reilly, M. M., Revesz, T., Booth, D. R., Booth, S. E., Hawkins, P. N., Pepys, M. B., and Morgan-Hughes, J. A. (1999) *Brain* **122,** 183–190
46. Kruger, R., Kuhn, W., Muller, T., Woitalla, D., Graeber, M., Kosel, S., Przuntek, H., Epplen, J. T., Schols, L., and Riess, O. (1998) *Nat. Genet.* **18,** 106–108
47. Kraulis, P. J. (1991) *J. Appl. Crystallogr.* **24,** 946–950

Downloaded from http://www.jbc.org/ at OSAKA UNIVERSITY on February 7, 2019

Amyloid Fibril Formation in the Context of Full-length Protein: EFFECTS OF PROLINE MUTATIONS ON THE AMYLOID FIBRIL FORMATION OF β 2-MICROGLOBULIN

Takeshi Chiba, Yoshihisa Hagihara, Takashi Higurashi, Kazuhiro Hasegawa, Hironobu Naiki and Yuji Goto

J. Biol. Chem. 2003, 278:47016-47024.
doi: 10.1074/jbc.M304473200 originally published online September 4, 2003

Access the most updated version of this article at doi: 10.1074/jbc.M304473200

Alerts:
- When this article is cited
- When a correction for this article is posted

Click here to choose from all of JBC's e-mail alerts

This article cites 47 references, 12 of which can be accessed free at
http://www.jbc.org/content/278/47/47016.full.html#ref-list-1

Downloaded from http://www.jbc.org/ at OSAKA UNIVERSITY on February 7, 2019